Improving the Balanced Coaxial Differential Probe for High-Voltage Pulse Measurements

Timothy J. Maloney (1), Dae-Hyung Cho (2), Steven S. Poon (3), and Boris Lisenker (4)

(1, 3-4) Intel Corporation, SC12-607, 2200 Mission College Blvd., Santa Clara, CA 95052 USA.
Tel. (408) 765-9389, Fax (408) 765-4716, e-mail: maloney@sc9.intel.com
(2) Intel Corporation, SC12-205, 2200 Mission College Blvd., Santa Clara, CA 95052 USA

Abstract **-** The balanced coaxial differential probe benefits from tuning of the probe and z-match inductances near the probe tip. Imbalances in the two channels can be assessed and minimized using a ferrite. The probe's network analyzer spectrum is explained, with common mode resonance over the cable length related to the main source of error.

I. Introduction

The operation and construction of the balanced coaxial differential probe has been described by Smith [1-3] and has proven to be useful in measuring fast high-voltage pulses related to EOS and ESD, usually operating up to at least 500 MHz. Because this probe is constructed entirely of passive components and includes no FETs, it is much more rugged than other oscilloscope probes in the presence of the high voltages that are associated with EOS and ESD.

The probe is constructed as Figure 1. Signals from the two probe points are divided down by the resistor network and launched along two transmission lines with a common shield. A 180-degree combiner [4,5] is used to subtract Channel 2 from Channel 1 and the difference signal goes into the 50-ohm scope input. This results in about 30X voltage reduction for the Mini-Circuits combiner [4] and 84X for the Barth combiner [5]. Smith [2] described the need for a 50-ohm match at the probe end in order to terminate backward-going waves, although the forward-going waves are well matched and isolated by the combiner circuit [4,5]. Our discussion of line coupling later will show even more clearly why this match is needed. Smith [2] also suggests that the series inductance of the 50-ohm impedance match at the probe end be reduced, by using four 200-ohm resistors as the match. We will show that the z-match inductance and the probe inductance (see Figure 2) are all part of a probe network that should be considered in its entirety.

In the remaining sections of the paper, we will first discuss circuit modeling of the probe tip (Fig. 2) and certain choices to be made in its design. Then we show how ferrite components can be used to raise the impedance of the unwanted common mode in various ways, including placement of a ferrite in front of the probe tips. We will see how ferrites can serve as a diagnostic check of probe construction and can possibly be a permanent part of the probe. Finally, we look at network analyzer data for probe gain from 50-550 MHz and view the probe as a pair of coupled transmission lines. It is shown that the differential probe resembles a certain class of directional couplers, which leads to a clearer view of the phenomena. Circuit modeling results explain much of the gain data over frequency, point out design limitations, and suggest ways to reduce the remaining imperfections in the differential probe.

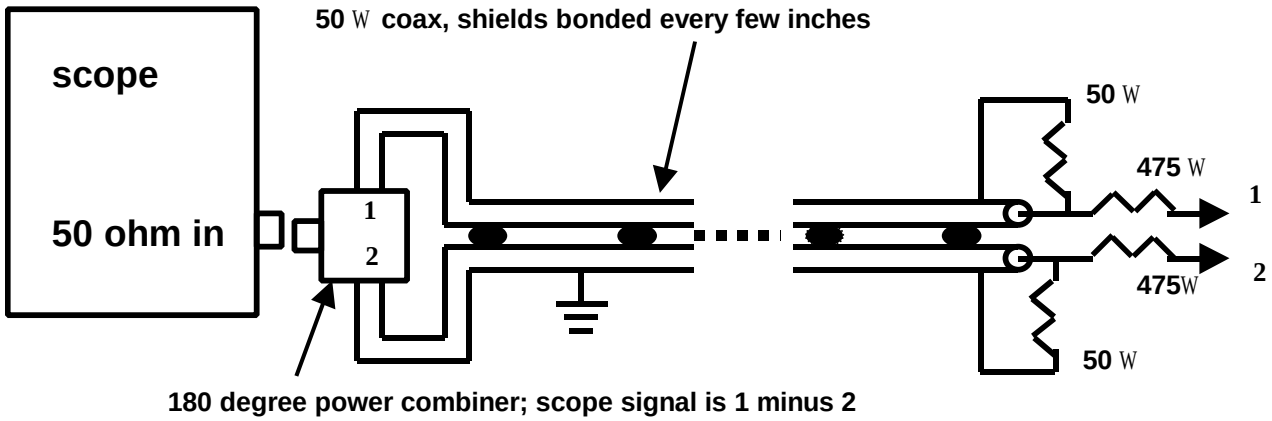

Figure 1. General scheme of coaxial probe, as described in Refs. 1-3.

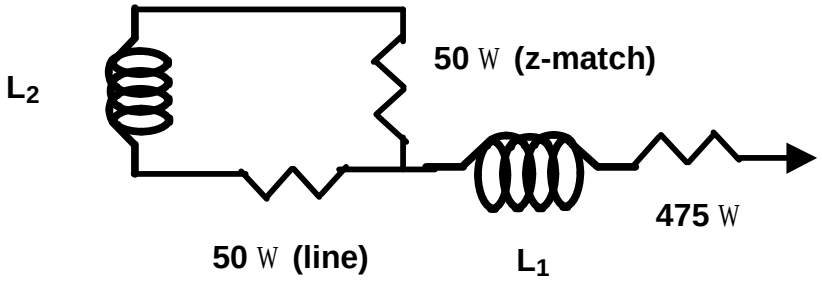

Figure 2. Equivalent circuit of one probe channel, with probe inductance (L_1) and z-match inductance (L_2) included.

II. Designing the Probe Tip Circuit

For each channel, we would like to calculate the voltage generated across the 50-ohm transmission line, which then enters the power combiner. The probe has 1000-ohms impedance, center-tapped to ground [1-3]. The resistors as shown in Figs. 1 and 2 achieve this and divide the voltage 20:1 (25 and 475-ohms) for low frequency, where the probe and z-match inductances can be ignored.

It is useful to examine the impact of the respective inductances on the gain, or transfer function, of the probe channels. We will see that this probe has matched L-R networks, as compared with more familiar matched R-C networks in other oscilloscope probes. The impedance looking into the terminated line section from the probe side is

$$Z = \frac{50(50 + jwL_2)}{100 + jwL_2}. \quad (1)$$

This is divided into the probe section impedance of $475 + jwL_1$ to give a gain for the probe channel of

$$G = \frac{\dfrac{50(1+jwt_2)}{2+jwt_2}}{\dfrac{50(1+jwt_2)}{2+jwt_2} + 475(1+jwt_1)}, \quad (2)$$

where $t_2 = \frac{L_2}{50}, t_1 = \frac{L_1}{475}$. Note that at low frequency, the probe gain, G, is 0.05 (20X). Equation 2 reduces to

$$G = \frac{50}{50 + \frac{475(1+jwt_1)(2+jwt_2)}{(1+jwt_2)}}. \quad (3)$$ For moderately small $\omega\tau_2$ this expands to

$$G = \frac{50}{50 + 475(1+jwt_1)(2+jwt_2)(1-jwt_2 - w^2t_2^2 + jw^3t_2^3 + ...)}. \quad (4)$$

Multiplying out the factors of 475 in the denominator, one then obtains

$$G = \frac{50}{50 + 475(2 + jw(2t_1 - t_2) + w^2t_2(t_1 - t_2) + O(w^3t^3))}. \quad (5)$$

These expressions suggest some interesting design points for the probe and z-match inductances L_1 and L_2, which determine τ_1 and τ_2. The z-match inductance L_2 is likely to be small but adjustable, while the probe inductance L_1 will be larger (as allowed by τ=L/R) yet is likely to have some minimum value, as it is often desired that the probe tip to end in a clip for convenient measurements.

For $\tau_1 = \tau_2$, the exact gain expression is

$$G = \frac{50}{50 + 475(2 + jwt)}. \quad (6)$$

There is a phase shift and slight gain degradation with frequency. An approximate expression is

$$G = 0.05(1 - 0.475jwt - 0.226w^2t^2 + ...). \quad (7)$$

Perhaps a more interesting design point occurs at $2\tau_1 = \tau_2$, where, in the expanded approximate expression above, the first order phase shift goes away and

$$G = \frac{50}{50 + 475(2 - 2w^2t_1^2 + O(w^3t^3))}, \quad (8) \text{ or}$$

$$G = 0.05(1 + 0.95w^2t_1^2 + ...). \quad (9)$$

So here the gain actually rises a little with frequency, without phase shift, and could possibly be used to compensate sources of high-frequency gain rolloff, starting with skin depth losses in the transmission lines. Of course, at some setting of τ_2 between τ_1 and $2\tau_1$ (very close to $(2\tau_1/\sqrt{3})$) there will be flat gain, to second order, with slight phase shift. Any of these design points are achievable if one considers τ_2 to be a consequence of the probe clip size, and τ_1 to be an adjustable load inductance.

A convenient rule of thumb for inductance is 10 nH per inch, although since loop area is important this is a very rough approximation. Note that, under the $2\tau_1 = \tau_2$ condition, 4 nH of z-match inductance then justifies 19 nH of probe tip inductance, enough for about 2 inches (5 cm) and sufficient for a small clip. But 4 nH in series with 50-ohms does not compromise the line matching too severely at 400-500 MHz, either, considering that the combiner box matching and port isolation is good.

III. Ferrite Experiments

With excellent common mode rejection by the combiner box [4,5], a major source of error in the differential probe is inductive imbalance in the two arms, as pointed out by Smith [3]. This error is hard to eliminate because the probe loop configuration changes each time. But the sensitivity to such errors can be reduced if the signal can be fed through a ferrite, as shown in Figure 3. The desired differential mode is "pre-selected" and passes through the ferrite unimpeded, while the common mode is heavily attenuated. The result is a truer reading of a transmission line pulse (TLP) rise time with the ferrite (Figure 4 curve 1) than without (curve 2). Without the ferrite, the inductive imbalance causes a false common mode (easily measured by shorting both probes to the top end of the TLP load), a false fast rise time and false waveform wiggle, as in Fig. 4 curve 2. These properties of unbalanced probe arms were also confirmed by circuit simulation, assuming that there is also some parasitic capacitance across the probe arms.

For investigative reasons, we solved a rather gross imbalance in probe arm inductance with Fig. 4. To confirm the Fig. 4 curve 1 result with the ferrite, we equalized the probe arm inductances well enough to obtain a smooth waveform very close to curve 2 of Fig. 4, but without using the ferrite. Thus the ferrite

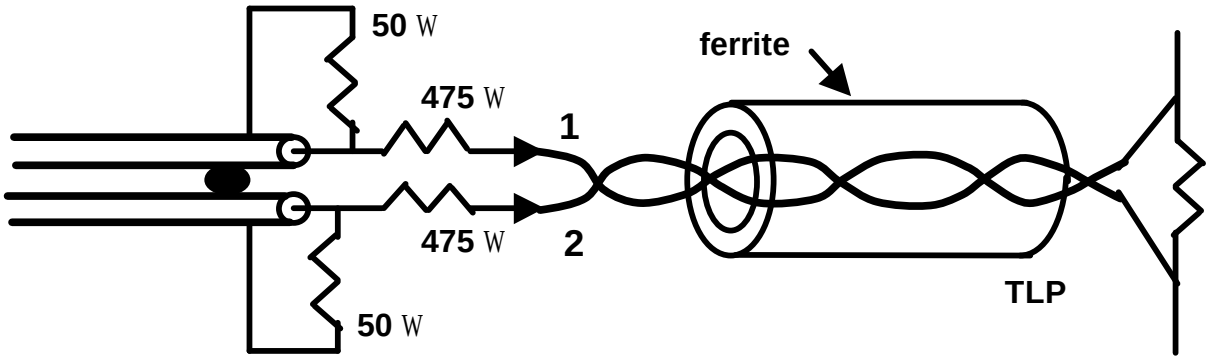

Figure 3. Feeding the sensed signal through a ferrite in order to assess imbalance in the channel 1 and 2 arms, or to reduce sensitivity to imbalance.

is a good way to eliminate the false common mode and obtain the best possible waveform with the balanced coaxial differential probe. In the same way, when a ferrite test shows little difference in waveforms, it proves that the arms are well balanced, and thus serves as a useful diagnostic test.

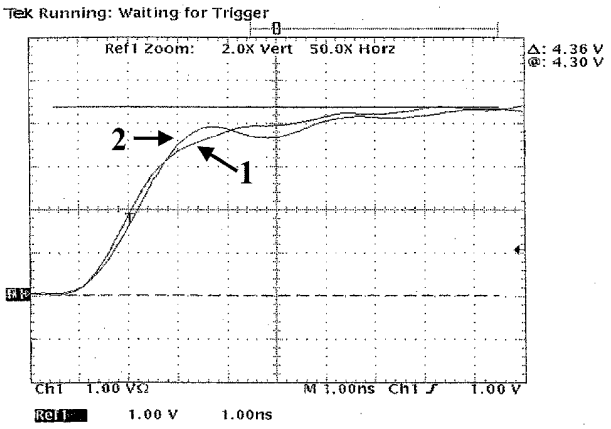

Figure 4. Rising edge of 300V 50-ohm TLP pulse across 50-ohm load as measured by 30X differential probe (30V/div) with poorly balanced channels. Rise time is smoother through a ferrite (curve 1) than without a ferrite (curve 2). Curve 1 agrees with the result for a well-balanced probe, without a ferrite.

The ferrite used for Figs. 3 and 4 is a Fair-Rite [6] model 266166-5702, over 25 mm long and weighing 20 grams. At that weight and length, it is not really suitable for permanent use on a differential probe.

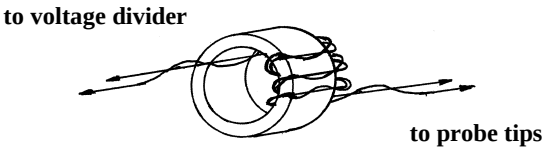

Figure 5. Toroidal wrapping of a small ferrite, for placement between the probe tips and the voltage divider.

However, if a smaller ferrite, such as Fair-Rite model 2643002401, is toroidally wrapped (Figure 5), it can be very effective. At 5 mm long and weighing just a few grams, it can be placed permanently at the front of a differential probe assembly. Results appear in the next section.

IV. High Frequency Probe Data and Analysis

In this section we present Network Analyzer S-parameter data for the differential probe, and explain some of its features with circuit simulations. As some aspects of the probe resemble a directional coupler, it will be useful to call upon coupled line theory and even-odd mode analysis to explain some of the high-frequency behavior.

IV.a. S-parameter data, 50-550 MHz, fully assembled probe

Network analyzer data for a differential probe are being presented for the first time, although Smith [1-3] noted the usefulness of such data. Figure 6 shows the voltage reduction factor, or multiplier, of the differential probe over the spectrum of interest, 50-550 MHz, using the Mini-Circuits combiner box [4]. The coaxial cable pair used was about 1.6 meters of RG 178B/U, with shields soldered together about every 3 inches (7-8 cm) as described by Smith. Measurements from 50-550 MHz were taken with an HP (Agilent) 8510C Network Analyzer, 83651 Synthesized Sweeper and 8517B S-parameter test set. With the probe on port 2 and the combiner on port 1, S12 in decibels (db)

is used to find the reciprocal gain, or voltage multiplier factor.

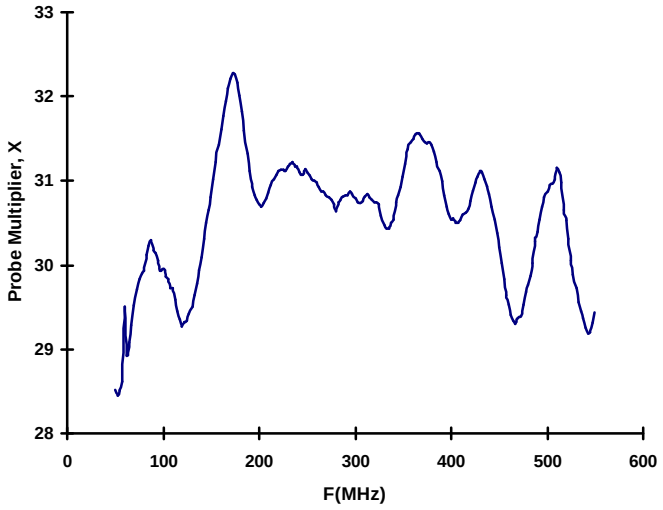

Figure 6. Probe voltage multiplier (X) vs. frequency, using Mini-Circuits combiner box. Variation is within 10%, or about 1 db.

To complement these results, probe performance from 1-50 MHz is easily observed with a waveform generator. Aside from the low-frequency cutoff of the combiner box, the voltage multiplier is about 30.5X over this entire range.

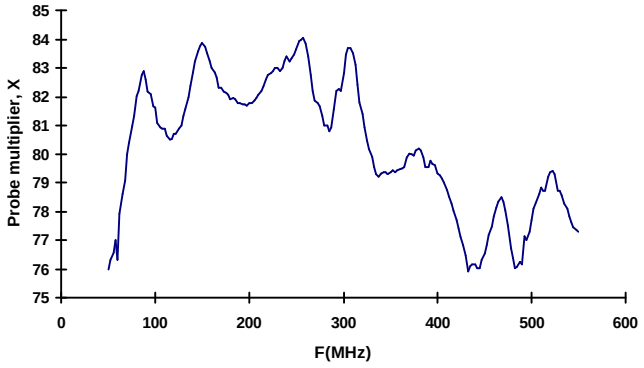

Figure 7. Probe voltage multiplier (X) vs. frequency, using Barth combiner box. Variation is <0.9 db and also within about 10%.

Figure 7 shows a comparable result for the same probe using the Barth combiner [5], but here the average probe multiplier is much higher because of more losses in the combiner. But the Barth combiner has more bandwidth at both ends (from kHz to GHz, rather than 1-500 MHz); this is evident at the top end of the frequency band, where the multiplier is lower, indicating a stronger signal. The scales of Figs. 6 and 7 have been blown up and truncated to show all details of the spectrum, but note that the performance of the probe over the range of interest is already pretty good. But there are periodic bumps in the spectrum, so we would like to explain them and minimize them.

A simple application of ferrites to the probe helped to smooth out the gain spectrum a perceptible amount. When several "snap-on" ferrites [6] were applied along the body of the probe (over the coaxial cables), the gain spectrum flattened slightly. A measure of this was that the standard deviation of the magnitude of the signal gain went from 0.25 db without the ferrites to 0.22 db with the ferrites.

Placing a ferrite near the front end of the probe, as in Fig. 5, had a more noticeable effect. Figure 8 compares data for such a probe to one with no ferrite (from Fig. 6), both using the Mini-Circuits combiner. The effect of the ferrite is to smooth out the variations over frequency, but the total variation is a little greater for the ferrite probe. We speculate that this performance could be improved by reducing the amount to which the ferrite also interferes with the differential mode, perhaps by using wires with thicker insulation. The ferrite spectrum itself is also important, of course, and one might improve over this one (the Fair-Rite 2643002401 mentioned earlier), selected from a small sampling.

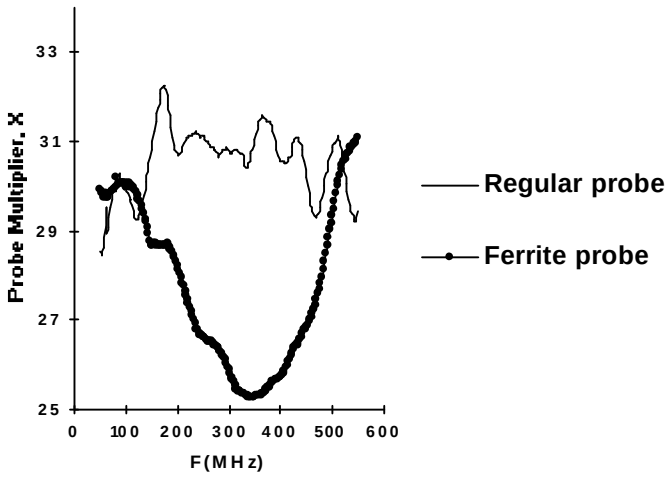

Figure 8. Probe voltage multiplier (X) vs. frequency, comparing regular probe (as in Fig. 6) with another probe having a ferrite up front, as in Fig. 5.

IV.b. Probe channel crosstalk data

The periodicity of the probe multiplier data over the frequency spectrum is an important clue. Major features every 45-90 MHz or so suggest that quarter-

wavelength and half-wavelength resonances of the entire 1.6m cable are involved. If the common cable shield is resonating in free space, then the two coaxial lines are coupled and it is appropriate to think of the problem in terms of crosstalk and directional couplers.

This is why we measured signal crosstalk between the two channels of the differential probe. Figure 8 shows the magnitude of the straight-through (Ch 1, 1A to 1B in Figure 9) and the crosstalk (Ch 2 far end, 1A to 2B in Fig. 9) signals. The signal is transferred to the other line (Ch 2) at odd numbers of quarter wavelengths (45 MHz, 135 MHz, etc.), while at integral half wavelengths (90 MHz, 180 MHz, etc.) the crosstalk is minimum. Phase information is not shown, but Ch 2 is generally 180 degrees out of phase with Ch 1, as expected for a largely undisturbed differential mode.

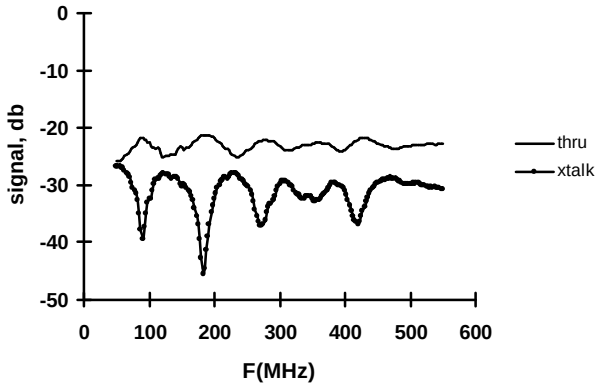

Figure 9. Signal strength vs. frequency for the two probe channels, showing effect of line coupling. Crosstalk is minimum where the cable length is an integral number of half wavelengths.

Fig. 9 begins to explain why the probe multiplier spectra look the way they do. A quick check of the data using the Microsoft Excel Fourier analysis tool confirms that the probe multiplier spectra in Figs. 6 and 7 do correlate strongly with the crosstalk spectrum in Fig. 9, as expected. But two other elements also contribute to the final differential voltage signal. One is the reflected signal at the input of Ch 1 (1A back on itself in Figure 10), the other is the near end crosstalk (backward coupled wave) into Ch 2 (1A to 2A in Fig. 10). These two can also be measured with the network analyzer, and are found to have about the same periodicity as the basic crosstalk signal in Fig. 9. They are nearly complementary to each other over frequency, as expected because each causes some loss of the final signal. But these signals do not all balance one another perfectly to create the differential output, that is why we are left with the variation of about 1 db shown in Figs. 6 and 7.

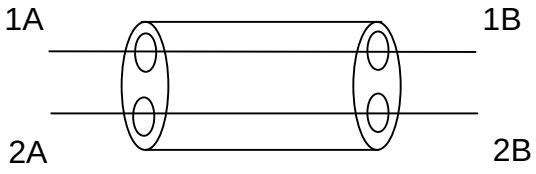

Figure 10. Simplified view of the probe as a four-port, with two coupled coaxial lines.

IV.c. Probe circuit model

The coaxial portion of the probe is modeled as two coaxial lines (50 ohms impedance each) with a common shield. The coupling results from the shield being suspended in space, meaning that the shield and its distributed capacitance to an external ground return form a third transmission line, one largely in air dielectric. A section of the distributed model is shown in Figure 11. In accordance with the probe design as in Fig. 1, the shield is open circuited at the probe end and short circuited to ground at the combiner and scope end. The "air line" is then excited by the common (even) mode [7] and results in coupling between the two coaxial lines, to be discussed below.

The properties of RG 178B/U cable easily give the distributed L and C values (240 nH/m, 96 pF/m) for Ch 1 and Ch 2, but it is less clear what to use for the constituents of the air line. We used values to give propagation at the speed of light with 250 ohms impedance.

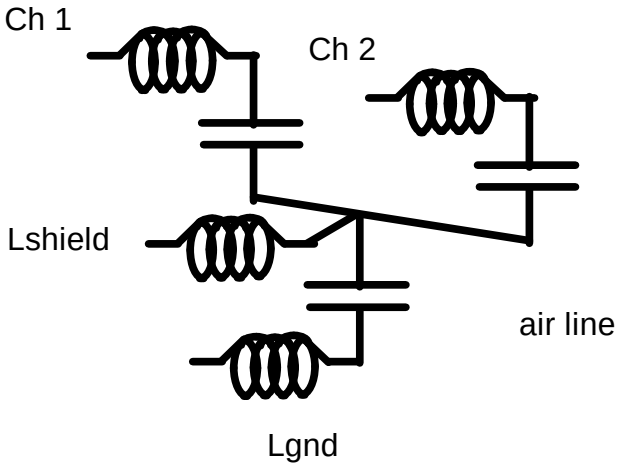

Figure 11. Section of distributed model of coupled coaxial lines of differential probe.

At this point we must invoke even and odd modes of coupled line excitation, as are often discussed in microwave texts [7]. The even (common) mode is the sum of the input signals V1+V2 and the odd mode is, of course, V1-V2, the voltage difference of the input signals. It is the differential mode, the odd mode, that we are trying to select with the entire probe assembly. We would like this to be a pure eigenmode of the coupled lines and insensitive to any even mode excitation, or else as close to that as possible.

It is not clear what to use for Lshield in Fig. 11, since it is shorted out by the electric wall in odd mode due to symmetry, and is not part of the 50 ohm odd mode impedance. We took Lshield=24 nH/m so that the even mode of the cables by themselves (were the cable shields to be the even mode return path) is not much changed from 50 ohms. As is often the case, it may not be possible to rigorously describe both even and odd mode with the same circuit model.

Using a circuit model with 80 sections of the Fig. 11 model representing 1.6 meters of cable, we simulated the effect of a single-ended signal into one channel of the probe, as was the case for the experimental crosstalk data of Fig. 9. The result is shown in Figure 12. Crosstalk occurs in this idealized model much as it does in the experimental data of Fig. 9. The peaks and dips of each line follow the experimental results very well, and the effect of air line resonance is clearly seen. But note the predicted crossover effect of Fig. 12, where the signal transferred to the other line ends up, at some frequencies, stronger than the remaining signal in the original line. We saw crossover effects like this in some crosstalk data, just not in the series shown in Fig. 9. We don't know the exact reason for the stronger measured signal in the main channel. The air line model of Fig. 11 could have too high an impedance, and may not properly account for the short cut in the ground return for the S-parameter test set, where port 1 and port 2 are much closer to each other than the length of the cable. But this configuration is an artifact of the network analyzer experiment, and perhaps less representative of real probe usage than the model used for Fig. 11.

V. Discussion

The coupled line portion of the differential probe bears a remarkable resemblance to a directional coupler structure attributed to S.B. Cohn, the re-entrant coupler [8,9]. Figure 13 shows the re-entrant cross-section and a top view of the coupler.

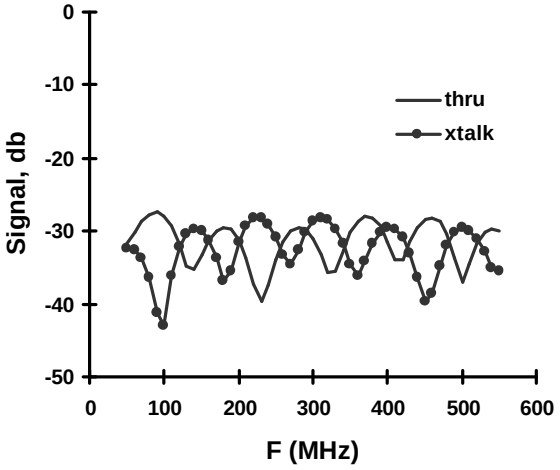

Figure 12. Simulated crosstalk from Ch 1 (thru) to Ch 2 (xtalk) using simple coupled line model with 80 segments as in Fig. 11; Compare with experimental data in Fig. 9.

Two shielded coaxial lines are suspended in a metal box that defines ground. As described in Refs. 8 and 9, the odd mode of the re-entrant coupler puts the cable shield at ground (electric wall) and has impedance $Z_{oo}=Z_{02}$ of the coaxial lines. The even mode puts each coaxial line in series with half the line between the shield and ground, Z_{01}, so the even mode impedance is $Z_{oe}=Z_{02}+2Z_{01}$. In accordance with directional coupler theory, the amount of coupling depends on the split between Z_{oo} and Z_{oe}, with coupling constant

$$k = \frac{Z_{oe} - Z_{oo}}{Z_{oe} + Z_{oo}} = \frac{Z_{01}}{Z_{01} + Z_{02}}. \quad (10)$$

With this equation in mind, the only way to have no line coupling at all is to have $Z_{01}=0$, which is hard to achieve unless the cable shields are several cubic meters of metal!

Note that there are some differences between the differential probe coaxial lines and the re-entrant coupler. One is that the differential probe shield is grounded at one end (the combiner box) and open at the probe end, while the re-entrant coupler's common shield is open at both ends. Another is that the differential probe is 50-ohm matched at all four ports, which matches the odd mode but not the even mode, while directional couplers are matched for optimized

coupling and directivity, with the external line impedance $Z_0 = \sqrt{Z_{oo} Z_{oe}}$ [7-9].

This coupled line view of the differential probe is very useful for understanding the crosstalk behavior as shown in Figs. 9 and 12. The coupling changes as the impedance of the shorted shield changes from the point of view of the probe input. At the half wavelength points for the air line, the shield short at the combiner transforms to a near-short at the probe input, thus the coupling is minimized because the effective $Z_{01} \approx 0$. The opposite effect happens at odd-quarter wavelength points and the coupling peaks, as also seen in Figs. 9 and 12.

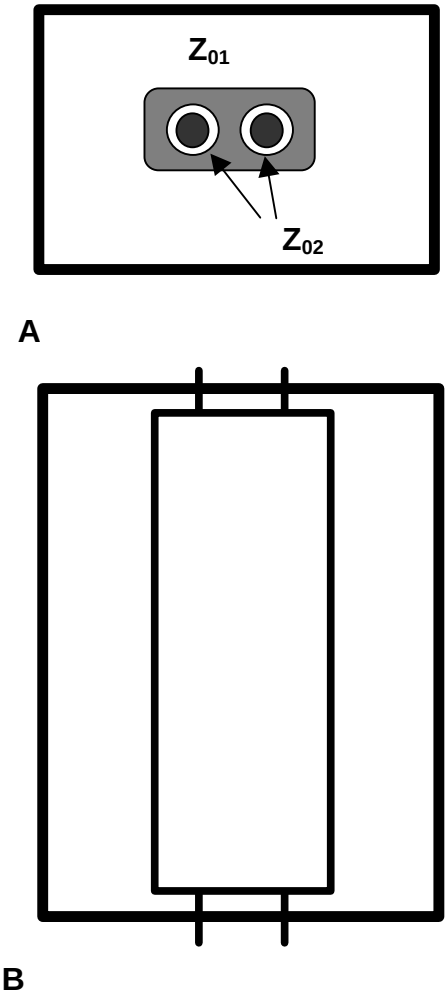

Figure 13. Re-entrant coupler [8,9]; (A) cross-sectional view, and (B) top view.

The coupling analysis can help point the way to improvements in the differential probe. While setting $Z_{01}=0$ with cubic meters of metal, as facetiously suggested earlier, is not practical, it is tempting to try to reduce coupling substantially by making Z_{01} as low as possible. With little coupling, perhaps variations will not make a difference. For that reason we tried a large-diameter braided shield over the cable to return the ground from combiner box to probe, and took network analyzer measurements. We were wary of how the even mode current would have to rise as a result of lower impedance, which proved crucial. We saw huge resonances at the 90 MHz marks, as shown in Figure 14, where the even mode current (and resulting flux density inside the braided shield) is at a maximum. This suggests some kind of effective even-odd mode coupling, the simplest reason for which would be unbalanced probe arms, where the even mode produces an odd mode probe input. True mode coupling could possibly be caused by mutual inductance in the tight 3-inch cable loops between the solder lumps. We tried several circuit models to describe this but never found one to explain all the s-parameter data, including the finding that an odd mode-only stimulus has the same spectrum as Fig. 14.

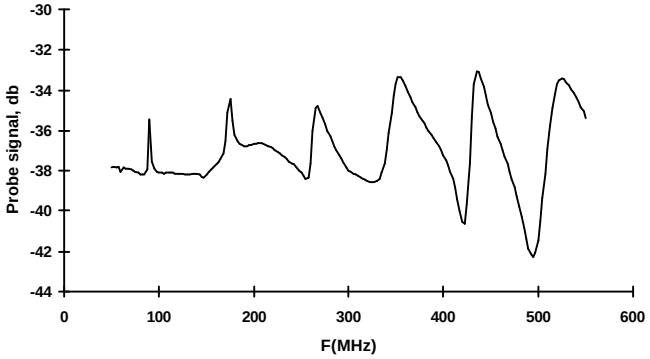

Figure 14. Differential probe signal spectrum with braided shield ground return from Barth combiner box to network analyzer probe ground at probe end. 90 MHz half-wavelength resonance series is seen.

Other experiments revealed no real improvement for quarter-wave stubs connected to the shield at various points—they could suppress resonance at one frequency but cause a resonance at a new frequency. The standard deviation of the frequency-dependent gain was about the same, but a little worse, than with no stubs. Much experimentation convinced us that the odd mode (difference) signal appears to be least affected when the even mode impedance is high. In this case, little even mode current flows. That explains the advantage of raising the even mode impedance with ferrites, as discussed earlier.

Circuit simulations of the coupled lines as in Fig. 11 were done, using 80 segments to describe a 1.6 meter pair of cables, much as in the simulations for Fig. 12. The probe inputs were identical resistive voltage dividers. With such a simple model, the odd/even mode separation is perfect, and the only way to observe any frequency dependence of the odd mode is to have a mismatch at either end, causing odd mode reflections and resonance. With this view we see the wisdom of adding 50 ohm matches at the probe end of the cable as introduced by Smith [2]. Odd mode reflections, and their time-delayed effect on the output signal, are suppressed as the backward-coupled waves become terminated.

Note that with this idealized model, the crosstalk occurs as in Fig. 12 but even-odd mixing does not. Therefore the crosstalk is a side effect only, not necessarily correlated to non-ideal probe gain. What the crosstalk does indicate is frequency-variant even mode impedance and line coupling, which turns out to be linked to non-ideal probe gain due to imperfections.

While an odd mode impedance mismatch by itself can explain the observed 1 db probe gain variation, it is unlikely that we have such a severe mismatch; our simulations indicate it would be as if 35 or 70 ohms terminated the 50 ohm lines. More likely the probe arms and voltage dividers are unbalanced just enough to produce some mode conversion at the input, that is, there is a limit to common mode rejection (CMR) in the probe arms. CMR is well engineered into the combiner boxes, but is more difficult to achieve in the moveable probe arms. For this reason, odd mode conversion reaches a peak at the even mode resonance points where the even mode current is highest. Then we have the same line-length related periodicity in the frequency domain as the crosstalk signal, although not all network analyzer data are explained this way. But once again, we conclude that reducing the even mode current, perhaps with the use of a ferrite, is the best strategy.

Note that there is a price to be paid for having long pairs of coaxial cables serving as the differential probe—the longer the cables, the more even mode resonances there will be, and starting at lower frequency. The low frequency resonances will also have higher Q, and thus will draw more even mode current. Shorter cables, if you can live with them, will be more accurate.

It is interesting to note certain other papers in the technical literature which treat coupled line situations similar to this. For example, the work of S. Sali looks at such distributed coupled line problems as the coupling between separated coaxial cables [10] and coupling in triaxial cable [11]. Common to them is the behavior at high frequency, both in theory and experiment, where singularities are observed as the full length of cable (usually 1 meter) goes through quarter and half-wave resonances, much as we have seen in this work.

VI. Summary and Conclusions

With the work of Smith [1-3], the balanced coaxial differential probe has reached an advanced state of development. But there are a few aspects of its design that are worthy of further scrutiny and publication, now treated in this paper.

There will always be some parasitic inductance in the probe arms as well as in the matched loads at that same end of the cables. In this work we have shown how this is a matter of balancing the inductances, because a little inductance in the line match helps to reduce frequency rolloff effects. With the relevant equations for a simple L-R model of the probe ends, we showed how about 2 inches (5 cm) of probe length justifies an extra 4 nH of inductance in the matched load.

The two coaxial lines in the differential probe behave like coupled lines in many ways. It is useful to consider signals on these lines in terms of even and odd (common and differential) modes. Our interest is in selecting the odd mode only, using a passive 180 degree combiner circuit. As the even mode is not useful to us and can interfere with the odd mode, it helps to minimize the amount of current in it by raising its impedance as much as possible. One way to do this, even on a temporary basis for checking the probe assembly, is to use ferrites to filter out the even mode before the signal reaches the probe's voltage divider. This is forgiving of slight errors and asymmetry in the probe channels. With a lightweight ferrite, toroidally wound, one can consider using it as part of the probe assembly, placed between the voltage dividers and the probe tips.

Network analyzer data show the probe gain, or voltage multiplier, over the frequency spectrum of interest, up to 550 MHz. Errors amount to only about 1 db, or

10% in voltage gain, but the spectrum correlates strongly with the quarter- and half-wavelength resonance series for the full cable length. It turns out that the coupling of the cables to each other is seen even more easily and varies with frequency in the same way. The strongest coupling is at quarter wavelength points, and the weakest at half-wavelength points, as expected from coupled line theory. This variable coupling is largely harmless as far as the differential signal is concerned, but since the even mode current varies, there is a variable amount of even-odd mode crossover due to imperfections in the lines. This is the origin of the probe gain variation, and the reason why we suggest minimizing the even mode current, i.e., keeping even mode impedance high.

Distributed circuit models have been useful for understanding the differential probe operation. We reproduced the crosstalk effects convincingly, and found several ways in which the probe gain can vary over frequency in the manner observed:

1. Matching the odd mode impedance at both ends of the cables is very important, or else time-delayed reflections will interfere with the main signal.
2. Balancing the two probe arms to have identical resistance and inductance is important because any imperfections will convert the even mode signal into a false odd mode signal.
3. Mutual inductance imperfections in the cable assembly can introduce frequency-dependent gain, so bonding the cable shields is indeed necessary. This is still under investigation and we are not sure of its relative importance once the shields are bonded in the usual way.

Further investigation of the balanced coaxial differential probe may reveal simple ways to remove the last vestiges of common mode resonance effects, and also extend the probe's range to higher frequency. As with this work, we expect coupled line theory and circuit modeling to contribute to any such improvements.

Acknowledgments

The authors thank Tina Cantarero for manuscript and figure preparation, and thank Andy Volk and Doug Barlage for technical review. They also thank Avner Schwarz, Artour Levin, Paul Packan and Avi Avraham for managerial support.

References

1. D.C. Smith, "Applying High Frequency Techniques to Measuring ESD Phenomena and its Effects", 1989 EOS/ESD Symposium Proceedings, EOS-11, pp. 114-119.
2. D.C. Smith, "Techniques and Methodologies for Making System Level ESD Response Measurements for Troubleshooting or Design Verification", 1992 EOS/ESD Symposium Proceedings, EOS-14, pp. 47-54.
3. D.C. Smith, "Balanced Probe Extends High-Frequency Measurements", IEEE Circuits and Devices, Nov. 1994, pp. 19-23.
4. Mini-Circuits combiner/splitter, ZFSCJ-2-1, see www.minicircuits.com.
5. Barth Electronics Model 691-MFBM, see www.barthelectronics.com.
6. Fair-Rite Products Corp., www.fair-rite.com.
7. D.M. Pozar, *Microwave Engineering* (New York: J. Wiley and Sons, 1998).
8. S.B. Cohn, "The Re-Entrant Cross Section and Wide-Band 3-db Hybrid Couplers", IEEE Trans. Microwave Theory and Techniques, vol. MTT-11, pp. 254-258, July 1963.
9. G. Matthaei, L. Young, and E.M.T. Jones, *Microwave Filters, Impedance-Matching Networks, and Coupling Structures* (New York: McGraw-Hill, 1964; reprinted by Artech House, 1980), pp. 798-800.
10. S. Sali, "A Circuit-Based Approach for Crosstalk Between Coaxial Cables with Optimum Braided Shields", IEEE Trans. On Electromagnetic Compatibility, vol. 35, May 1993, pp. 300-311.
11. S. Sali, "Screening Efficiency of Triaxial Cables with Optimum Braided Shields", IEEE Trans. On Electromagnetic Compatibility, vol. 32, May 1990, pp. 125-136.